PHYSICAL REVIEW A VOLUME 39, NUMBER 7 APRIL 1, 1989

Fractal measures of passively convected vector fields and scalar gradients in chaotic fluid flows

Edward Ott and Thomas M. Antonsen, Jr.
Laboratory for Plasma Research, Department of Electrical Engineering,
and Department of Physics and Astronomy, University of Maryland, College Park, Maryland 20742
(Received 15 August 1988; revised manuscript received 19 December 1988)

The passive convection of vector fields and scalar functions by a prescribed incompressible fluid flow $\mathbf{v}(\mathbf{x},t)$ is considered for the case where $\mathbf{v}(\mathbf{x},t)$ is chaotic. By chaotic $\mathbf{v}(\mathbf{x},t)$ it is meant that typical nearby fluid elements diverge from each other exponentially in time. It is shown that in such cases, as time increases, a convected vector field and the gradient of a convected scalar will generally concentrate on a set which is fractal. The present paper relates the stretching properties of the flow to the resulting fractal dimension spectrum. Motivation for these considerations is provided by the kinematic magnetic dynamo problem (in the vector case) and (in the scalar case) by recent experiments which demonstrate the possibility of measuring the fractal dimension of the gradient squared of convected passive scalars.

I. INTRODUCTION

In this paper we consider the convection of a vector field $\mathbf{B}(\mathbf{x},t)$ or a scalar function $\phi(\mathbf{x},t)$ by a chaotic incompressible flow.[1] That is, if $\mathbf{x}(t)$ denotes the trajectory of a fluid element,

$$\frac{d\mathbf{x}}{dt}=\mathbf{v}(\mathbf{x}(t),t)\ , \tag{1}$$

where $\mathbf{v}(\mathbf{x},t)$ is the fluid velocity, then $\mathbf{B}$ and ϕ satisfy the equations

$$\frac{d\mathbf{B}}{dt}=\mathbf{B}\cdot\nabla\mathbf{v} \tag{2a}$$

and

$$\frac{d\phi}{dt}=0\ , \tag{2b}$$

following a fluid element (i.e., $d/dt=\partial/\partial t+\mathbf{v}\cdot\nabla$). We assume that $\mathbf{v}(\mathbf{x},t)$ is determined by external dynamics, such as stirring, thermally induced convection, etc. The evolution of $\mathbf{B}$ and ϕ are assumed to have no influence on $\mathbf{v}(\mathbf{x},t)$, which we henceforth treat as prescribed.

The vectors $\mathbf{B}$ and $\nabla\phi$ have the property that their magnitudes grow due to local divergence of nearby fluid elements. That $|\mathbf{B}|$ grows in proportion to the local divergence follows from taking a linear variation of Eq. (1):

$$d\delta\mathbf{x}/dt=\delta\mathbf{x}\cdot\nabla\mathbf{v}\ , \tag{3}$$

which is the same as the equation for $\mathbf{B}$, Eq. (2a). We presume $\mathbf{v}(\mathbf{x},t)$ is a specified smooth function of $\mathbf{x}$, and we call the flow chaotic if (1) has ergodic regions with positive Lyapunov exponent, $h>0$, where

$$h=\lim_{t\to\infty}\ln[|\delta\mathbf{x}(t)|/|\delta\mathbf{x}(0)|]\ .$$

In Eulerian variables (2a) is

$$\frac{\partial\mathbf{B}}{\partial t}+\mathbf{v}\cdot\nabla\mathbf{B}=\mathbf{B}\cdot\nabla\mathbf{v}\ . \tag{4}$$

Equation (4) is the equation satisfied by the magnetic field in an incompressible perfectly conducting fluid. In this connection Eq. (4) has been studied with prescribed $\mathbf{v}(\mathbf{x},t)$ by Finn and Ott,[2,3] who were interested in the singular nature of the high-conductivity limit of the kinematic dynamo problem.[4] The kinematic dynamo problem may be stated as follows: given a prescribed flow of a conducting fluid, will a small seed magnetic field grow exponentially with time? If the answer is yes, then the flow tends to generate a magnetic field from small initial magnetic perturbations. Considering the astrophysical medium to be a flowing plasma, the kinematic dynamo problem is of basic interest in that it addresses the question of *why* magnetic fields occur in the universe (e.g., in stars, interplanetary, interstellar, and intergalactic space). In Refs. 2 and 3 it was shown that three-dimensional chaotic flows generally yield dynamos in the high-conductivity limit and that the magnetic flux tends to concentrate on a fractal set. What occurs is that the magnetic field following a typical fluid element will tend to grow exponentially. Some fluid elements, however, will have magnetic field growth which is larger than others. As a result of this nonuniform growth, as time proceeds, the largest magnetic field vectors will be contained in a smaller and smaller volume of space. In the zero-resistivity case and the limit $t\to\infty$ the volume of the set containing most of the magnetic flux shrinks to zero, and this limit set is highly singular in nature. In fact, it is a fractal set characterized by a noninteger dimension (actually, a spectrum of dimensions as described in Sec. II). The occurrence of fractal attracting sets is a well-known property for nonconservative flows in phase space[5] (strange attractors). Here a time asymptotic fractal set results for a *conservative* system (an *incompressible* flow). Note, however, that the fractal here attracts the flux of the convected vector field rather than typical orbits.

In addition, we also note that Eq. (4) is the equation satisfied by the vorticity in an incompressible inviscid fluid flow. Thus the considerations here may also be of interest for the study of high-Reynolds-number fluid turbulence. We note, in this connection, however, that, for the fluid turbulence case, the equation is extremely nonlinear, since the vorticity is the curl of $\mathbf{v}$, whereas for the kinematic dynamo $\mathbf{v}$ is prescribed and Eq. (4) is linear in $\mathbf{B}$. Furthermore, in the high-Reynolds-number limit of fluid turbulence $\mathbf{v}(\mathbf{x},t)$ is not a smooth function of $\mathbf{x}$ since $\nabla\times\mathbf{v}$ concentrates on a fractal.[6] Since in that which follows we will take $\mathbf{v}(\mathbf{x},t)$ as a prescribed smooth function, our considerations apply more directly to the dynamo problem. We speculate, however, that the methods used in this paper may yet be extendable to the more difficult, self-consistent fluid turbulence problem.

Considering the case of convection of the scalar ϕ, we see that the growth of $\nabla\phi$ due to divergence of nearby fluid elements follows from the fact that the difference between the values of ϕ on two adjacent fluid trajectories is a constant. That is,

$$\frac{d}{dt}(\delta\mathbf{x}\cdot\nabla\phi)=0 . \tag{5}$$

Since the flow is incompressible and chaotic, at least one solution for $\delta\mathbf{x}(t)$ must decrease in time as another grows. Consequently, $\nabla\phi$ must grow to maintain $\delta\mathbf{x}\cdot\nabla\phi$ constant. By analogy with the work on the vector case,[2,3] we can anticipate that nonuniform growth of $|\nabla\phi|$ will lead $\nabla\phi$ to concentrate on a fractal as well. The possibility of measuring the fractal dimensions of passive scalar gradients is demonstrated by the experiments in Ref. 7.

The relationship between the solutions of Eq. (3) and the vectors $\mathbf{B}$ and $\nabla\phi$ can be made more precise by considering the following. In three dimensions Eq. (3) will have three independent solutions for the linearized displacement $\delta\mathbf{x}$ about a trajectory: $\delta\mathbf{x}_1$, $\delta\mathbf{x}_2$, and $\delta\mathbf{x}_3$. If we represent the vector $\mathbf{B}$ in the basis formed by these vectors,

$$\mathbf{B}=\beta_1\,\delta\mathbf{x}_1+\beta_2\,\delta\mathbf{x}_2+\beta_3\,\delta\mathbf{x}_3 , \tag{6a}$$

Eq. (2a) implies that the (contravariant) coefficients β_1, β_2, and β_3 are constant along the trajectory of a fluid element. On the other hand, if we express the vector $\nabla\phi$ in terms of the reciprocal basis,

$$\nabla\phi=\alpha_1\,\delta\mathbf{x}_2\times\delta\mathbf{x}_3+\alpha_2\,\delta\mathbf{x}_3\times\delta\mathbf{x}_1+\alpha_3\,\delta\mathbf{x}_1\times\delta\mathbf{x}_2 , \tag{6b}$$

the (covariant) coefficients α_1, α_2, and α_3 are constants along the fluid trajectory. This follows by forming $\delta\mathbf{x}_i\cdot\nabla\phi$ and noting that the volume of the parallelepiped formed by $\delta\mathbf{x}_1$, $\delta\mathbf{x}_2$, $\delta\mathbf{x}_3$, namely,

$$\delta V=\delta\mathbf{x}_3\cdot\delta\mathbf{x}_1\times\delta\mathbf{x}_2=\delta\mathbf{x}_2\cdot\delta\mathbf{x}_3\times\delta\mathbf{x}_1=\delta\mathbf{x}_1\cdot\delta\mathbf{x}_2\times\delta\mathbf{x}_3 ,$$

is constant for incompressible flow.

The goal of this paper will be to relate the spectrum of fractal dimensions associated with the sets on which the vectors $\mathbf{B}$ and $\nabla\phi$ accumulate to properties of the chaotic flow. To this end it is first necessary to define measures μ whose fractal dimensions can be determined. We assume that the flow and the convected quantities are confined to a finite volume V_0 of space. For any subregion V in V_0, we define the measures $\mu_B(t,\gamma;V)$ and $\mu_\phi(t,\gamma;V)$ as

$$\mu_B=\frac{\int_V|\mathbf{B}(\mathbf{x},t)|^\gamma\,d^3\mathbf{x}}{\int_{V_0}|\mathbf{B}(\mathbf{x},t)|^\gamma\,d^3\mathbf{x}} , \tag{7a}$$

$$\mu_\phi=\frac{\int_V|\nabla\phi|^\gamma\,d^3\mathbf{x}}{\int_{V_0}|\nabla\phi|^\gamma\,d^3\mathbf{x}} , \tag{7b}$$

where $\mathbf{B}$ and ϕ are the solutions to Eqs. (2a) and (2b), respectively, with smooth initial conditions. [For our purposes, in what follows, we may think of $\mathbf{B}(\mathbf{x},0)$ and $\nabla\phi(\mathbf{x},0)$ as uniform fields.]

We suppose that if we examine Eq. (7) at some instant of time, $t=t_1$, then, if t_1 is sufficiently large, the measures μ_B and μ_ϕ will approximate fractal measures (cf. Sec. II). That is, if μ_B and μ_ϕ are examined with finite length resolution r, they look like fractal measures. *Ideally* r can be made as small as we please by making t_1 larger. In physical (nonideal) cases, however, we cannot make t_1 too large and still neglect the effects of diffusive processes. In the case of the dynamo, the magnetic field diffuses due to the finite electrical conductivity of real plasmas;[2-4] while for the passive scalar problem, the "contaminant" ϕ can diffuse through the convecting fluid.[7] Let r_{t1} be the typical small scale generated at time $t=t_1$ from Eqs. (2) (i.e., without diffusive processes). Let r_d be the minimum gradient scale set by diffusive processes in the limit $t_1\to\infty$. If t_1 is too large, then $r_{t1}<r_d$, and the diffusion cannot be ignored. Throughout most of this paper (except for Sec. V), we shall use Eqs. (2). Hence we assume that t_1 is an intermediate time long enough that r_{t1} is much less than the scale size of the flow (thus the concept of an approximate fractal is useful) yet short enough that $r_{t1}>r_d$ [thus diffusion can be neglected and Eqs. (2) apply].

It is our goal in this paper to relate the fractal dimension of the large-t measures to averages involving expansion and contraction rates of tangent vectors of the flow. In Sec. II we review concepts of dimension for a measure. If a dimension associated with a measure is noninteger we say that the measure is a fractal measure. In Sec. III we consider incompressible two-dimensional flows $\mathbf{v}(\mathbf{x},t)$ [i.e., if z denotes the third direction $\mathbf{v}(\mathbf{x},t)$ has no z component and is independent of z]. Section III A derives a partition function formalism which relates the stretching properties of the flow to the dimension spectrum of the long-time measures μ_B and μ_ϕ. It turns out that for two-dimensional flows the dimension spectra for μ_B and μ_ϕ are the same. The assumptions and validity of the partition function formalism are also discussed. Section III B applies the results of Sec. III A to a particular simple example, an incompressible generalized baker's map.[5] It is shown for this example that the partition function gives correct results (i.e., results in agreement with those derived by the similarity method, Ref. 3). Also it is evident from this example that fractal measures are to be expected in typical situations (i.e., flows where the stretching is nonuniform so that some fluid elements experience greater stretching than others). Section III C considers a formulation in terms of the distribution function for Lyapunov numbers. Section III D treats a model of a nonperiodic (e.g., turbulent or temporally chaotic) flow in terms of a random map. In this case, at each discrete time the map is to be applied, a parameter in the map is chosen at random. A possible analogy with spin glasses is pointed out in this case. Sections IV A and IV B derive the partition function formalisms for three-dimensional flows for the vector and scalar gradient cases, respectively. The treatment is very similar to that in Sec. III A, with the important difference that the dimension spectra for the vector and scalar gradient cases no longer coincide with each other when the flow is three dimensional. Section IV C applies the results of Secs. IV A and IV B to a specific $\mathbf{v}(\mathbf{x},t)$ which is smooth in space. For the particular $\mathbf{v}(\mathbf{x},t)$ we choose it is possible to carry out the stretching averages to determine an explicit analytical formula for the dimension. In Sec. V we consider the effect of nonideal diffusive processes on the vector and scalar problems. These effects can lead to important qualitative changes in the results of Secs. III and IV when t_1 becomes too large. Section VI concludes the paper.

II. DIMENSION OF A MEASURE

The spectrum of dimensions for a measure μ introduced by Renyi and later, in the context of nonlinear dynamics, by Grassberger and by Hentshel and Procaccia is given by the following formula:[8]

$$\hat{D}_q = \frac{1}{q-1} \lim_{\varepsilon\to 0} \left[\frac{\ln \sum_i \mu_i^q}{\ln \varepsilon} \right] , \tag{8}$$

where the quantity q is an index, $-\infty < q < +\infty$. Here we imagine the d-dimensional space in which the measure lies to be divided up by a cubic grid of grid size ε, and μ_i denotes the measure in the ith cube of the grid. Letting $q\to 0$, Eq. (8) becomes the capacity dimension

$$\hat{D}_0 = \lim_{\varepsilon\to 0} \left[\frac{\ln N(\varepsilon)}{\ln(1/\varepsilon)} \right] , \tag{9}$$

where $N(\varepsilon)$ is the number of cubes in the grid needed to cover the set. Letting $q\to 1$ Eq. (8) becomes

$$\hat{D}_1 = \lim_{\varepsilon\to 0} \left[\frac{\sum_i \mu_i \ln \mu_i}{\ln \varepsilon} \right] , \tag{10}$$

which is called the information dimension.[5] Grassberger and Halsey *et al.*[9] have introduced a variant on Eq. (8) which allows the measure to be covered by a set of cubes of variable sizes. Specifically they define the following quantity (called the partition function):

$$\Gamma(\tau,q,\varepsilon,\{S_i\}) = \sum_i \frac{\mu_i^q}{\varepsilon_i^\tau} , \tag{11a}$$

where $\{S_i\}$ denotes a set of cubes of edge lengths $\varepsilon_i \le \varepsilon$ which cover the measure, μ_i is the measure in cube i, and $\tau \equiv (q-1)D$. If $q<1$ $(q>1)$ we choose the set of cubes $\{S_i\}$ so as to make Γ as small (large) as possible subject to the constraint $\varepsilon_i \le \varepsilon$,

$$\Gamma(\tau,q,\varepsilon) = \begin{cases} \text{minimum over } \{S_i\} \text{ of } \Gamma(\tau,q,\varepsilon,\{S_i\}) & \text{if } q<1 \\ \text{maximum over } \{S_i\} \text{ of } \Gamma(\tau,q,\varepsilon,\{S_i\}) & \text{if } q>1 . \end{cases} \tag{11b}$$

We then take the limit $\varepsilon\to 0$,

$$\Gamma(\tau,q) = \lim_{\varepsilon\to 0} \Gamma(\tau,q,\varepsilon) . \tag{11c}$$

It can be shown that Γ will then be infinite if τ exceeds a critical value, and Γ will be zero if τ is less than this critical value,

$$\Gamma(\tau,q) = \begin{cases} 0 & \text{if } \tau<\tau_q \\ \infty & \text{if } \tau>\tau_q , \end{cases} \tag{12}$$

where we have denoted the critical value of τ by τ_q. A dimension D_q is then defined by

$$D_q = \tau_q/(q-1) . \tag{13}$$

If the set $\{S_i\}$ were taken as the cubes in a grid, and the optimization specified by Eq. (11b) were ignored, then the dimension definitions of $\hat{D}_q$ and D_q would be the same. The optimization (11b) can, in principle, make D_q smaller than $\hat{D}_q$,

$$D_q \le \hat{D}_q . \tag{14}$$

III. DIMENSION FOR TWO-DIMENSIONAL INCOMPRESSIBLE FLUID MOTIONS

A. Partition function from stretching properties of the system

We first consider the case where the continuous flow is modeled by a two-dimensional area-preserving map. This is appropriate for time-periodic flows in two dimensions if the map is continuous. In addition, as shown in Refs. 2 and 3, a discontinuous, two-dimensional map can model a smooth time-periodic three-dimensional flow whose action in each time period is to nonuniformly stretch, twist, and fold the fluid.

In the case of a time-periodic flow one imagines integrating Eq. (1) over a period of the flow to obtain a recursion relation or map,

$$\mathbf{x}_{n+1} = \mathbf{M}(\mathbf{x}_n) , \tag{15}$$

where $\mathbf{x}_n$ is the position of a fluid element at the end of the nth time period of the flow. A variation of this equation,

$$\delta \mathbf{x}_{n+1} = \underline{J}(\mathbf{x}_n)\cdot\delta\mathbf{x}_n \ , \tag{16}$$

where $\underline{J}$ is the Jacobian matrix of partial derivatives of $\mathbf{M}$, produces the linearized trajectories $\delta\mathbf{x}_n$ from which the evolution of the vectors $\mathbf{B}$ and $\nabla\phi$ can be deduced. [Equation (16) is the map version of Eq. (3).] In the case of two dimensions ($\partial/\partial z \equiv 0$) considered in this section, we may take one of the $\delta\mathbf{x}_i$ to be in the third direction (which we take to be the z direction), and Eq. (6) becomes

$$\mathbf{B} = \beta_1\,\delta\mathbf{x}_1 + \beta_2\,\delta\mathbf{x}_2 \ ,$$

$$\nabla\phi = \alpha_1\,\delta\mathbf{x}_1 \times \mathbf{z}_0 + \alpha_2\,\delta\mathbf{x}_2 \times \mathbf{z}_0 \ .$$

Thus, if $\delta\mathbf{x}_1$ grows exponentially, we see that $|\mathbf{B}| \sim |\nabla\phi| \sim |\delta\mathbf{x}_1|$. From this it follows that in two-dimensional chaotic flows μ_B and μ_ϕ typically concentrate on the same fractal set. Thus in what follows it suffices to consider only μ_B.

Although our discussion in this section is in the context of smooth maps appropriate to time-periodic two-dimensional flows, we emphasize that there is no formal difference in treating flows with nonperiodic time dependence. In that case we can imagine strobing the flow periodically in time. The only resulting difference would be that the function $\mathbf{M}$ in Eq. (15) would become an explicit function of time, $\mathbf{M} = \mathbf{M}(\mathbf{x}_n, n)$. An example of this type where the dependence on n is random (i.e., $\mathbf{M}$ is chosen randomly from some probability distribution at each iterate) is given in Sec. III D. This randomness in the map might be interpreted as a crude model for a turbulent flow.

In order to find the dimension of the measure in Eq. (7a) in terms of Lyapunov numbers, we use a technique previously utilized for chaotic attractors and chaotic repellers of dissipative dynamical systems.[10,11] Suppose we start at $t=0$ with a uniform field $\mathbf{B}(\mathbf{x},0) = \mathbf{B}_0$ and imagine that we divide the space by a square grid of unit grid size δ. We now iterate the map n steps. If δ is small enough, the action of the map on a given square will be linear. Thus the map will take an initial square into a parallelogram. Let $\lambda_{1j}^n \equiv L_{1j}$ and $\lambda_{2j}^n \equiv L_{2j}$ be the magnitudes of the eigenvalues of the Jacobian matrix of the n times iterated map for initial conditions in the jth square, where $\lambda_{1j}^n > 1 > \lambda_{2j}^n$ (note that $\lambda_{1j}\lambda_{2j} = 1$ since areas are preserved). Then the parallelogram will be long and thin, with long dimension $\lambda_{1j}^n\delta$ and short dimension $\lambda_{2j}^n\delta$, as shown in Fig. 1 (where the parallelogram has been drawn as a rectangle). We then cover the resulting parallelogram with smaller boxes of edge length $\lambda_{2j}^n\delta$. There are roughly $\lambda_{1j}^n/\lambda_{2j}^n = \lambda_{1j}^{2n}$ such boxes. Let μ_j denote the measure initially in box j. Let $\hat{\mu}_j$ denote the measure in one of the small boxes covering the j parallelogram at iterate n. Since the fields have been increased by a factor λ_{1j}^n due to stretching, and the area of a little box is smaller than the area of box j by a factor $\lambda_{2j}^{2n} = \lambda_{1j}^{-2n}$, we have from Eq. (7a)

$$\hat{\mu}_j = \frac{\mu_j \lambda_{1j}^{(\gamma-2)n}}{\sum_j \mu_j \lambda_{1j}^{\gamma n}} \ ,$$

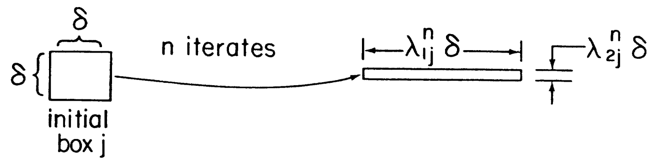

FIG. 1. n iterates of the jth box.

where, in the sum in the denominator, we have taken into account the fact that the parallelogram is covered by λ_{1j}^{2n} small boxes. For a uniform initial field, all the μ_j are equal and we obtain

$$\hat{\mu}_j = \frac{L_{1j}^{(\gamma-2)}}{\sum_j L_{1j}^{\gamma}} \ , \tag{17}$$

where $L_{1j} = \lambda_{1j}^n$. From Eq. (11)

$$\Gamma = \sum_j L_{1j}^2 \frac{\hat{\mu}_j^q}{\varepsilon_j^\tau} \ ,$$

where $\varepsilon_j = \delta/L_{1j} \sim L_{1j}^{-1}$. Inserting Eq. (17) then yields

$$\Gamma \sim \left[\sum_j L_{1j}^{[(q-1)(D-2)+\gamma q]}\right] \Big/ \left[\sum_j L_{1j}^{\gamma}\right]^q . \tag{18}$$

We thus define a new partition function based on the stretching properties of the map,

$$\Gamma_\lambda(D,q,n) \equiv \langle L_1^\sigma \rangle / \langle L_1^\gamma \rangle^q \ , \tag{19a}$$

$$\sigma \equiv (q-1)(D-2) + \gamma q \ , \tag{19b}$$

where $L_1(\mathbf{x})$ is the largest Lyapunov number of the n times iterated map for the orbit originating at the point $\mathbf{x}$, and the angle brackets denote an average over space[12] (i.e., over $\mathbf{x}$). Letting $n \to \infty$ in Eq. (19) is analogous to letting $\varepsilon \to 0$ in Eq. (11c) (recall that for Fig. 1, $\varepsilon_i = \delta/\lambda_{1j}^n$). Thus we define a dimension $\tilde{D}_q$ as the value of D at which the quantity

$$\Gamma_\lambda(D,q) = \lim_{n\to\infty} \Gamma_\lambda(D,q,n) \tag{20}$$

goes from zero to infinity as $(q-1)D$ increases. Again, since the optimization specified by Eq. (11b) has not been carried out,

$$\tilde{D}_q \geq D_q \ . \tag{21}$$

However, it appears to us that our covering is a rather natural one, and we conjecture that (at least for hyperbolic maps) the equality in Eq. (21) applies. Indeed this will be shown to be the case for the generalized baker's map example in Sec. III B.

We can obtain an explicit *parametric* representation of the function $\tilde{D}_q$ versus q as follows. For large n we approximate $\tilde{D}_q$ as the solution of $\Gamma_\lambda(D,q,n) = 1$ (since for n large the quantity Γ_λ passes from very large values to very small values as D passes through $\tilde{D}_q$). Equations (19a) and (19b) then yield

$$q(\sigma) = \lim_{n\to\infty} \frac{\ln\langle L_1^\sigma \rangle}{\ln\langle L_1^\gamma \rangle} \ ,$$

$$\tilde{D}_q(\sigma)=2+(\sigma-\gamma q)/(q-1)\ .$$

Thus, from the first equation, we obtain a value of q for each value of σ which when inserted in the second equation yields the corresponding $\tilde{D}_q$. Numerical computations of $\tilde{D}_q$ versus q based on this procedure should be fairly efficient.

It is of interest to investigate Eq. (19) for several limiting cases.

(i) For $q=0$, Eq. (19) yields $\Gamma_\lambda=\langle L_1^{(2-D)}\rangle$. Since $L_1\to\infty$ as $n\to\infty$, we have $\tilde{D}_0=2$. The interpretation is that there is an area such that *any* subset S_0 of this area which itself has positive area has $\mu(\gamma,S_0)>0$.

(ii) For $\gamma=0$, we have $\Gamma_\lambda=\langle L_1^{(q-1)(D-2)}\rangle$ which again yields $\tilde{D}_q=2$.

(iii) Perhaps the most interesting case is the limit $q\to 1$. Equation (19) gives to first order in $(q-1)$ the result,

$$\Gamma_\lambda=1+(q-1)\left[(D-2+\gamma)\frac{\langle L_1^\gamma \ln L_1\rangle}{\langle L_1^\gamma\rangle}-\ln\langle L_1^\gamma\rangle\right]\ .$$

For $n\to\infty$ we have

$$\frac{\langle L_1^\gamma \ln L_1\rangle}{\langle L_1^\gamma\rangle}\sim\ln\langle L_1^\gamma\rangle\sim n\ .$$

Thus the coefficient of the $(q-1)$ term in Γ_λ becomes large with n unless $D=\tilde{D}_1$ with

$$\tilde{D}_1=2-\gamma\lim_{n\to\infty}\frac{\langle L_1^\gamma \ln L_1^\gamma\rangle-\langle L_1^\gamma\rangle\ln\langle L_1^\gamma\rangle}{\langle L_1^\gamma \ln L_1^\gamma\rangle}\ . \tag{22}$$

Note that for any function $f(x)$ of a variable x, where $d^2f/dx^2\geq 0$, we have $\overline{f(x)}\geq f(\bar{x})$, where the overbar denotes an average over x. Thus, with $f(x)=x\ln x$, we obtain

$$\langle L_1^\gamma \ln L_1^\gamma\rangle\geq\langle L_1^\gamma\rangle\ln\langle L_1^\gamma\rangle\ ,$$

and hence $\tilde{D}_1\leq 2$. The equality is attained only if all the L_1 in the average are the same. That is, the distribution function for L_1 (cf. Sec. III C) is a δ function. Hence, if the stretching is nonuniform, then $\tilde{D}_1<2$ and the measure is, in general, fractal. The example of Sec. III B clearly shows this.

For the case of a smooth two-dimensional flow (rather than a discrete map), all the considerations above carry through with L_i replaced by $\exp(h_i t)$ where h_i is the Lyapunov exponent calculated for the given initial condition in the time interval 0 to t, and t denotes the continuous time variable replacing the discrete time variable n.

Our considerations above assume a splitting between distinct expanding and contracting directions (cf. Fig. 1), as well as ergodic behavior of orbits throughout some region of space. Thus our considerations would be expected to apply to time-periodic flows if the dynamics is hyperbolic (such cases have, by definition, the splitting mentioned above). Note, in particular, that Kol'mogorov-Arnol'd-Moser (KAM) tori are absent in hyperbolic processes. For nonhyperbolic cases, without discernible KAM tori, we might also expect the theory of this section to be relevant. For example, at a large nonlinearity parameter the standard map and the *ABC* map (Sec. IV) are of this type. The latter case is treated in Sec. IV. More generally, in flows which are not steady or periodic in time (e.g., turbulent or temporally chaotic flows) there are no KAM tori (the concept in these cases does not even make sense), and we expect our partition function to apply. At any rate, nonperiodic time dependence is probably a case of great interest, since many flows encountered in practice are of this type. In addition, we note that related partition functions based on local stretching rates have been constructed for determining the dimension spectra of strange attractors of dynamical systems.[10,11] In this case, current evidence strongly suggests that these partition functions give correct dimension spectra even for nonhyperbolic processes provided that q is not too large, $q<q_T$, where q_T is a critical value.[11] From an analogy with thermodynamics the behavior at q_T has been shown to correspond to a phase transition.[11] If such phenomena also occur for the case of chaotic time dependence of the flow $\mathbf{v}(\mathbf{x},t)$ then the situation might be analogous to a phase transition in a spin glass[13] (cf. Sec. III D).

B. Example: the generalized baker's map

To make matters more concrete we consider a particular example of a two-dimensional map, the incompressible, generalized baker's map,[2,3,5]

$$x_{n+1}=\begin{cases}\alpha x_n & \text{if } y_n<\alpha\\ 1-\beta x_n & \text{if } y_n>\alpha\ ,\end{cases} \tag{23a}$$

$$y_{n+1}=\begin{cases}y_n/\alpha & \text{if } y_n<\alpha\\ (1-y_n)/\beta & \text{if } y_n>\alpha\ ,\end{cases} \tag{23b}$$

where $\alpha+\beta=1$. The action of this map on the unit square is illustrated in Fig. 2. The unit square is divided by a horizontal line at $y=\alpha$. The lower rectangle is compressed in the x direction by a factor α and expanded in the y direction by a factor $1/\alpha$ and placed in the left side of the unit square. The upper rectangle is compressed in the x direction by a factor $\beta=1-\alpha$, expanded in the y direction by a factor $1/\beta$, and then inverted top to bottom and left to right and placed on the right side of the unit square. The inversion is such that the side originally located at $x=0$ winds up at $x=1$, and the side originally located at $y=1$ winds up at $y=0$. Strictly speaking this map is not continuous. However, if

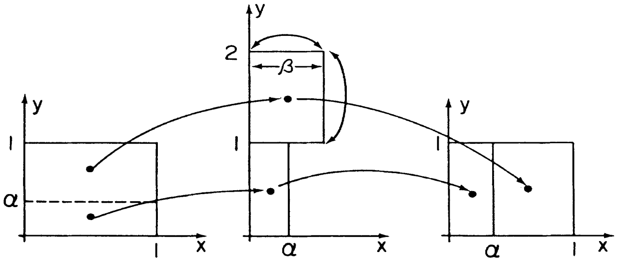

FIG. 2. Schematic illustrating the generalized baker's map examined in Sec. III B.

we select as initial conditions

$$\mathbf{B}(x,y,\, n=0)=\hat{\mathbf{y}}B_0$$

and

$$\phi(x,y,\, n=0)=x\Phi_0 \ ,$$

then all quantities will remain independent of y, and no singularities in the fields, $\mathbf{B}$ and $\nabla\phi$, develop as a result of the discontinuities in the map. In particular, ϕ remains continuous.

We now consider what application of the map does to the fields $\mathbf{B}$ and $\nabla\phi$. After one iteration of the map we have two strips: one $(0<x<\alpha)$ with $|\mathbf{B}|/B_0=|\nabla\phi|/\phi_0=\alpha^{-1}$ and one $(\alpha<x<1)$ with $|\mathbf{B}|/B_0=|\nabla\phi|/\phi_0=\beta^{-1}$. After a second iteration there will be four strips, two of width $\alpha\beta$ with vector field strengths proportional to $(\alpha\beta)^{-1}$ and one each of widths α^2 and β^2 with field strengths proportional to α^{-2} and β^{-2}, respectively. After n applications, we have 2^n strips of varying widths, $\alpha^{n-m}\beta^m$ $(m=0,1,2,\ldots,n)$, and field intensities, $(\alpha^{m-n}\beta^{-m})$. The number of strips corresponding to a given m is the binomial coefficient,[3,5]

$$Z(m,n)=n!/[m!(n-m)!] \ .$$

In general, the fields are increasing with time everywhere. However, if the stretching is nonuniform, $\alpha\neq\beta$, the rate of increase is larger for some orbits than for others. The result is that the measure of the fields defined by Eqs. (7) takes on the character of a fractal set, emphasizing the points where the growth is largest.

Let us now perform the averages defined in Eq. (19). The appropriate weighting function to be assigned to an initial condition that results in a sequence which has m contractions by α and $n-m$ contractions by β is

$$P(m,n)=\alpha^m\beta^{n-m}Z(m,n) \ ,$$

where $\alpha^m\beta^{n-m}$ represents the area of the initial conditions that will experience a particular sequence of contractions, and the factor $Z=n!/[m!(n-m)!]$ accounts for the number of such sequences. For particular values of m and n, the magnitude of the largest eigenvalue of the Jacobian of the n times iterated map corresponding to that sequence is

$$L_1(m,n)=\alpha^{-m}\beta^{-(n-m)} \ .$$

Thus we find

$$\langle L_1^\nu\rangle=\sum_{m=0}^{n}P(m,n)(\alpha^{-\nu m}\beta^{-\nu(n-m)}) \ , \qquad (24)$$

or, using the binomial identity,

$$\langle L_1^\nu\rangle=\left[\alpha\left[\frac{1}{\alpha}\right]^\nu+\beta\left[\frac{1}{\beta}\right]^\nu\right]^n \ . \qquad (25)$$

The partition function can then be written directly in closed form,

$$\Gamma_\lambda=\frac{(\alpha^{1-\sigma}+\beta^{1-\sigma})^n}{(\alpha^{1-\gamma}+\beta^{1-\gamma})^{qn}} \ , \qquad (26)$$

where σ is given in Eq. (19b). As $n\to\infty$, Γ_λ will either go to zero or diverge depending on σ. The critical value which defines $D_q(\gamma)$ is the solution of the transcendental equation,

$$\alpha^{1-\sigma}+\beta^{1-\sigma}=(\alpha^{1-\gamma}+\beta^{1-\gamma})^q \ . \qquad (27)$$

This same result has been derived in Ref. 3 using similarity arguments. The fact that Eq. (27) derived using the partition function (19) agrees with Ref. 3 is a confirmation of the correctness of Eq. (19) for hyperbolic cases. As an example, let $q\to1$ and $\gamma=1$. Then Eq. (27) yields

$$\tilde{D}_1=1+\frac{\ln2}{\ln[1/(\alpha\beta)^{1/2}]} \ ,$$

which is less than 2 (and hence indicates a fractal) if $\alpha\neq\beta=(1-\alpha)$ (i.e., $\alpha\neq\frac{1}{2}$). [This follows since the maximum value of $\alpha(1-\alpha)$ is $\frac{1}{4}$ and occurs at $\alpha=\frac{1}{2}$.] For $\alpha=\frac{1}{2}$ all initial conditions experience precisely the same stretching $(1/\alpha=1/\beta=2)$ on each iterate. For general chaotic flows, nonuniform stretching is to be expected. Thus for typical situations we expect fractal measures.

C. Distribution function of Lyapunov exponents

The analytical result (27) is obtained easily in the example under consideration because we have made use of the binomial identity to simplify the partition function. Suppose instead that we attempted to evaluate the average in Eq. (24) directly. To this end we introduce the distribution of Lyapunov exponents (cf., for example, Grassberger *et al.*[11]) implied by $P(n,m)$. Let

$$L(m,n)=\exp[nh(m,n)]=(\alpha^m\beta^{n-m})^{-1} \ , \qquad (28)$$

where h is the Lyapunov exponent. As $n\to\infty$ the discrete sum over m can be replaced by a continuous integral over h,

$$\sum_m P(m,n)L^\nu=\int_0^\infty dh\, p(h,n)e^{\nu nh} \ . \qquad (29)$$

Using the explicit expression for $L(m,n)$, Eq. (28), and approximating $Z(m,n)$ for large n and m by using Sterling's formula, we find

$$p(h,n)=[nG''(h)/2\pi]^{1/2}\exp[-nG(h)] \ , \qquad (30)$$

where

$$G(h)=\hat{m}\ln\hat{m}+(1-\hat{m})\ln(1-\hat{m})+\hat{m}\ln(\beta/\alpha)-\ln\beta \ , \qquad (31)$$

with

$$\hat{m}=(h+\ln\beta)/\ln(\beta/\alpha) \ .$$

Thus, as $n\to\infty$, the distribution of exponents becomes peaked about $\bar{h}$ where

$$G'(\bar{h})=0 \ ,$$

with a width that decreases as $n^{-1/2}$. We can now perform the integral in Eq. (29) using the method of steepest descent to obtain

$$\langle L^\nu\rangle=\exp\{-n[G(\xi_\nu)-\nu\xi_\nu]\} \ ,$$

where ξ_ν is defined by the condition for the exponent to be stationary,

$$G'(\xi_\nu)=\nu \; . \tag{32}$$

Using this result in the partition function results in the expression

$$\Gamma_\lambda=\frac{\exp\{-n[G(\xi_\sigma)-\sigma\xi_\sigma]\}}{\exp\{-nq[G(\xi_\gamma)-\gamma\xi_\sigma]\}} \; . \tag{33}$$

Thus the condition for Γ_λ to be finite as $n\to\infty$ is

$$G(\xi_\sigma)-\sigma\xi_\sigma=q[G(\xi_\gamma)-\gamma\xi_\gamma] \; . \tag{34}$$

It can be verified for the particular case of G given by Eq. (31) that Eqs. (27) and (34) are equivalent as they should be.

We now argue that the result (34) is general for typical two-dimensional maps. That is, in typical cases Eq. (30) describes the distribution of Lyapunov exponents with the functional dependence of G different for different maps. As a result, there is an implicit relation between the spectrum of fractal dimensions $D_q(\gamma)$ and the distribution of exponents $\sim\exp(-nG)$. Further, because $D_q(\gamma)$ is determined by a single function G, the functional dependence of D on the two parameters γ and q is restricted. We note, however, that this will not be the case in three dimensions (Sec. IV).

D. Random maps

The specific example of Sec. III B, i.e., the generalized baker's map, was taken as a model for a time-periodic flow. We now consider as a model of nonperiodic flows a further generalization of the map described by Eqs. (23) where we allow the parameters α and $\beta=1-\alpha$ to be different on each iteration. Further, we imagine that at each iteration the value of α is selected randomly according to some distribution $P_0(\alpha)$. For a given realization, the distribution function for Lyapunov exponents satisfies the recursion relation

$$\begin{aligned}p(n+1,h)=&\ \alpha_n p(n,[(n+1)h-\ln\alpha_n^{-1}]/n)\\ &+\beta_n p(n,[(n+1)h-\ln\beta_n^{-1}]/n) \; ,\end{aligned} \tag{35}$$

where α_n and $\beta_n=(1-\alpha_n)$ are the parameters for the $(n+1)$th iteration of the map. We assume that, for large n and for each realization, the distribution function tends to the form given by Eq. (30), where $G(h)$ will have an average value $\bar{G}(h)$ (which is independent of n and the same for all realizations) and a small fluctuation δG_n (which is different from realization to realization and varies with n). Inserting $G=\bar{G}+\delta G_n$ in the recursion relation (35) and expanding for n large and δG_n small, we obtain

$$\begin{aligned}n[\delta G_{n+1}(h)-\delta G_n(h)]+\bar{G}(h)-h\bar{G}'(h)&\\ =-\ln(\alpha_n^{1-\bar{G}'}+\beta_n^{1-\bar{G}'}) \; ,&\end{aligned} \tag{36}$$

where $\bar{G}'(h)=d\bar{G}/dh$. Averaging Eq. (36) produces a transcendental differential equation for $\bar{G}(h)$,

$$\bar{G}(h)-h\bar{G}'(h)=-\int_0^1 d\alpha\, P_0(\alpha)\ln(\alpha^{1-\bar{G}'}+\beta^{1-\bar{G}'}) \; . \tag{37}$$

Further, one can see that as $n\to\infty$ the deviation δG_n will tend to zero as $n^{-1/2}$, justifying the current approach.

While Eq. (37) is difficult to solve explicitly for $G(h)$ we can immediately obtain a transcendental equation for the dimension $D_q(\gamma)$. In particular, the condition for a stationary exponent in the steepest-descent integration, Eq. (32), determines the value of $\bar{G}'(h)$, and the value of the integral itself is dependent on the combination $\bar{G}-h\bar{G}'$. Thus Eq. (34) can be written

$$\int_0^1 d\alpha\, P_0(\alpha)[\ln(\alpha^{1-\sigma}+\beta^{1-\sigma})-q\ln(\alpha^{1-\gamma}+\beta^{1-\gamma})]=0 \; , \tag{38}$$

from which the fractal dimension is determined.

Equation (38) could have been determined more directly by using the binomial identity to express the partition function Γ_λ,

$$\Gamma_\lambda=\frac{\prod_n(\alpha_n^{1-\sigma}+\beta_n^{1-\sigma})}{\prod_n(\alpha_n^{1-\gamma}+\beta_n^{1-\gamma})^q} \; .$$

As $n\to\infty$ the partition function will tend to zero or infinity exponentially unless $\sigma(q)$ assumes the critical value which determines $D_q(\gamma)$. Thus we anticipate that in general for large n,

$$\Gamma_\lambda=\exp[nF_n(\sigma,\gamma,q)] \; ,$$

where the function F_n will have average value $\bar{F}$ plus a small deviation. The critical value of σ can then be determined by demanding that the average of the logarithm of the partition function vanish as $n\to\infty$,

$$\bar{F}=\frac{1}{n}\overline{\ln\Gamma_\lambda}=0 \; . \tag{39}$$

We believe Eq. (39) has general relevance and can be used, for example, for low-Reynolds-number turbulent flows. Equation (39) has a formal similarity to the problem of spin glasses. There one considers a random Hamiltonian (analogous to our random sequence) and is again interested in the average of the logarithm of the partition function.[13]

IV. DIMENSION SPECTRA FOR THREE-DIMENSIONAL INCOMPRESSIBLE FLUID MOTIONS

In this section we consider fully three-dimensional fluid flows. Unlike the two-dimensional case treated in Sec. III, in the three-dimensional case the partition function for the measure of a convected vector [μ_B given in Eq. (7a)] and the partition function for the gradient of a convected scalar [μ_ϕ given in Eq. (7b)] are unequal. Section IV A obtains the partition functions for the vector case, while Sec. IV B treats the case of a convected scalar. In both cases the resulting dimensions are strictly upper bounds on the box counting dimension [one can also deal with "partial dimension" associated with different directions as in the case of chaotic attractors (cf. Grassberger and co-workers[9,11])]. Section IV C presents results for a particular flow (the *ABC* map) as an illustration of the utility of these results.

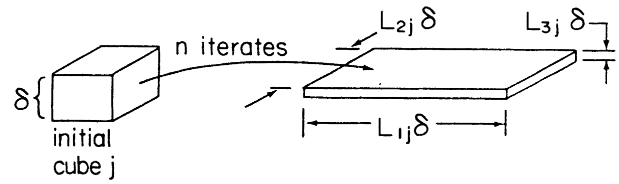

FIG. 3. *n* iterates of the *j*th cube.

A. Partition function for convected vector fields

We proceed as in Sec. III A, except that now we have three (rather than two) Lyapunov numbers $\lambda_{1j} \geq \lambda_{2j} \geq \lambda_{3j}$ with $\lambda_{1j}\lambda_{2j}\lambda_{3j}=1$, and now the subscript j labels a cube in a three-dimensional grid of unit size δ (see Fig. 3). In this case we must give some partial attention to the optimization specified by Eq. (11b). In particular, we can consider covering the slab at the nth iterate in Fig. 3 either with cubes of edge length $L_{3j}\delta$ or with cubes of edge length $L_{2j}\delta$. In order to decide between these choices, we invoke (11b), and use the choice which gives the larger Γ_λ when $q>1$ and the smaller Γ_λ when $q<1$. Covering with cubes of edge $L_{3j}\delta$, we have

$$\Gamma_{\lambda 3}=\langle L_1^{\gamma q} L_3^{-(q-1)(D-3)}\rangle / \langle L_1^{\gamma}\rangle^q \,. \tag{40a}$$

Covering with boxes of edge $L_{2j}\delta$, we have

$$\Gamma_{\lambda 2}=\langle L_1^{\gamma q}(L_2^{(D-2)} L_3^{-1})^{-(q-1)}\rangle / \langle L_1^{\gamma}\rangle^q \,. \tag{40b}$$

Comparing Eqs. (40a) and (40b), we see that they are equal at $D=2$ and that by virtue of the definition of L_2 and L_3 (i.e., $L_2 \geq L_3$)

$$\Gamma_{\lambda 2} \gtrless \Gamma_{\lambda 3} \text{ if } (D-2)(q-1) \gtrless 0 \,.$$

Thus

$$\Gamma_\lambda=\begin{cases}\Gamma_{\lambda 2} & \text{if } D \leq 2 \\ \Gamma_{\lambda 3} & \text{if } D \geq 2 \,,\end{cases} \tag{41}$$

and $\tilde{D}_q$ is defined to be the value of D at which $\lim_{n\to\infty}\Gamma_\lambda$ passes from zero to infinity. Again Γ_λ gives an upper bound on the dimension, $\tilde{D}_q \geq D_q$.

For the case of a continuous time system (a flow), as opposed to a map, the Lyapunov numbers $L_1 \geq L_2 \geq L_3$ may be replaced by $L_r \to \exp(h_r t)$ $(r=1,2,3)$, where $h_1(\mathbf{x},t) \geq h_2(\mathbf{x},t) \geq h_3(\mathbf{x},t)$ are the Lyapunov exponents computed for the time interval between 0 and t for the orbit whose initial condition is $\mathbf{x}$. In particular, note that for the case of a time-independent flow $h_2=1$.

For $q \to 1$, Eqs. (40) and (41) give

$$\tilde{D}_1=\min\begin{cases} 3-\lim\limits_{n\to\infty}\left[\dfrac{\langle L_1^{\gamma}\ln L_1^{\gamma}\rangle-\langle L_1^{\gamma}\rangle\ln\langle L_1^{\gamma}\rangle}{\langle L_1^{\gamma}\ln(L_1L_2)\rangle}\right] & \text{(42a)}\\ 2+\lim\limits_{n\to\infty}\left[\dfrac{\langle L_1^{\gamma}\ln L_1^{\gamma}\rangle-\langle L_1^{\gamma}\rangle\ln\langle L_1^{\gamma}\rangle+\langle L_1^{\gamma}\ln L_3\rangle}{\langle L_1^{\gamma}\ln L_2\rangle}\right] \,. & \text{(42b)}\end{cases}$$

B. Partition function for the gradient of a passively convected scalar

The growth of a convected vector following a fluid element is $\sim L_1$. That is, the vector grows in proportion to its stretching. The growth of the gradient of a passively convected scalar following a fluid element is $\sim L_3^{-1}$. That is, the gradient grows in proportion to how much nearby points become still nearer. Since ϕ is conserved following fluid elements, the exponential approach of nearby points implies exponential growth of $\nabla\phi$. Thus now $|\nabla\phi|^\gamma \sim L_{3j}^{-\gamma}$ in computing the measure in Eq. (7b). [In Sec. III we had $|\nabla\phi|^\gamma \sim L_{2j}^{-\gamma}=L_{1j}^{\gamma}$ (where $L_{1j}L_{2j}=1$ by incompressibility) which rendered the results for $\nabla\phi$ and $\mathbf{B}$ identical. In three-dimensional flows we have $L_{1j}L_{2j}L_{3j}=1$, and so there is no clear relation between the results for $\nabla\phi$ and $\mathbf{B}$.] Proceeding as in Secs. III A and IV A, but using $|\nabla\phi|^\gamma \sim L_{3j}^{-\gamma}$ in place of $|\mathbf{B}|^\gamma \sim L_{1j}^{\gamma}$, we obtain the following results:

$$\Gamma_{\lambda 3}=\langle L_3^{-\gamma q+(q-1)(3-D)}\rangle / \langle L_3^{-\gamma}\rangle^q \,, \tag{43a}$$

$$\Gamma_{\lambda 2}=\frac{\langle L_2^{1+(q-1)(3-D)} L_3^{-(\gamma q+1)}\rangle}{\langle L_2 L_3^{-(1+\gamma)}\rangle^q} \,, \tag{43b}$$

where if $\tilde{D}_q$ is calculated from both Eqs. (43a) and (43b) we choose the smaller of the two. Letting $q \to 1$ in Eq. (43) gives

$$\tilde{D}_1=\min\begin{cases} 3-\gamma\lim\limits_{n\to\infty}\left[1-\dfrac{\langle L_3^{-\gamma}\rangle\ln\langle L_3^{-\gamma}\rangle}{\langle L_3^{-\gamma}\ln L_3^{-\gamma}\rangle}\right] & \text{(44a)}\\ 3+\lim\limits_{n\to\infty}\left[\dfrac{\langle L_2L_3^{-(\gamma+1)}\ln L_3^{-\gamma}\rangle-\langle L_2L_3^{-(\gamma+1)}\rangle\ln\langle L_2L_3^{-(1+\gamma)}\rangle}{\langle L_2L_3^{-(\gamma+1)}\ln L_2\rangle}\right] \,. & \text{(44b)}\end{cases}$$

C. An example: The *ABC* map

We consider a particular fluid velocity given by

$$\mathbf{v}(\mathbf{x},t)=\mathbf{x}_0\tilde{v}_x(y,z)\delta_T(t-\varepsilon)+\mathbf{y}_0\tilde{v}_y(x,z)\delta_T(t-2\varepsilon)+\mathbf{z}_0\tilde{v}_z(x,y)\delta_T(t-3\varepsilon)\ , \tag{45}$$

where δ_T is a periodic string of δ functions,

$$\delta_T(t)=T\sum_{n=-\infty}^{+\infty}\delta(t-nT)\ ,$$

and ε is a small positive quantity. Integrating $d\mathbf{x}/dt=\mathbf{v}(\mathbf{x},t)$ through one period T, we obtain a three-dimensional volume-preserving map which relates $\mathbf{x}$ at time $t=nT$ to $\mathbf{x}$ at time $t=(n+1)T$,

$$\begin{aligned} x_{n+1}&=x_n+T\tilde{v}_x(y_n,z_n)\ ,\\ y_{n+1}&=y_n+T\tilde{v}_y(x_{n+1},z_n)\ ,\\ z_{n+1}&=z_n+T\tilde{v}_z(x_{n+1},z_{n+1})\ . \end{aligned} \tag{46}$$

Letting $T\to 0$, Eqs. (45) and (46) go over to the steady continuous flow $\mathbf{v}(\mathbf{x},t)=\tilde{v}_x(y,z)\mathbf{x}_0+\tilde{v}_y(x,z)\mathbf{y}_0+\tilde{v}_z(x,y)\mathbf{z}_0$. Here we consider finite T and choose the so-called *ABC* form for $\tilde{v}_x$, $\tilde{v}_y$, $\tilde{v}_z$,

$$\begin{aligned} \tilde{v}_x&=A\ \sin z+C\cos y\ ,\\ \tilde{v}_y&=B\ \sin x+A\ \cos z\ ,\\ \tilde{v}_z&=C\ \sin y+B\ \cos x\ . \end{aligned} \tag{47}$$

This choice has been extensively studied as an example of a chaotic flow in the case of a steady flow $(T\to 0)$ by Dombre *et al.*[1] More recently, the "*ABC* map" given by Eqs. (46) and (47) has been introduced.[2,3,14] Here we study the map version with the parameters chosen so that $AT=BT=CT\equiv K$ and K is large. As an example, we calculate the information dimension of the measure of a convected vector field μ_B by using the partition function given in Eq. (42) [for this map Γ_λ can also be evaluated from Eq. (40)]. Using reasoning similar to that used by Chirikov[15] to calculate the Lyapunov number of the standard map with large nonlinearity parameter (analogous to large K in the above), we will be able to calculate the various Lyapunov number averages appearing in Eq. (42).

For the special case we consider, the map is

$$\begin{aligned} x_{n+1}&=x_n+K(\cos y_n+\sin z_n)\ ,\\ y_{n+1}&=y_n+K(\sin x_{n+1}+\cos z_n)\ ,\\ z_{n+1}&=z_n+K(\cos x_{n+1}+\sin y_{n+1})\ . \end{aligned} \tag{48}$$

Linearizing Eq. (48) for small variations $\delta\mathbf{x}_n$ about an orbit $\mathbf{x}_n$ [cf. Eq. (16)], we find that to lowest significant order in a large-K expansion of Eq. (48),

$$\delta z_{n+1}\cong K^3\cos x_{n+1}\cos y_{n+1}\cos z_n\ \delta z_n\ .$$

Let $\eta_n=\cos x_{n+1}\cos y_{n+1}\cos z_n$. Then we have

$$|\delta z_n|/|\delta z_0|\cong K^{3n}|\eta_{n-1}\eta_{n-2}\cdots\eta_1\eta_0|\ . \tag{49}$$

Following Chirikov's treatment of the standard map, we note that, for large K, Eq. (48) produces displacements which are typically large compared to the periodicity length of the map [$K\gg$(periodicity length)$=2\pi$]. Thus the correlation time of the chaotic orbit is approximately zero. In particular, when averaging Eq. (49) over initial conditions we may neglect correlations between η_n and η_m $(n\neq m)$. Using this, we can perform the averages in Eq. (42a) [it turns out that $\tilde{D}_1>2$, so Eq. (42a) rather than Eq. (42b) is relevant] as follows:

$$\langle L_1^\gamma\rangle\cong K^{3\gamma n}I_1^{3n}\ ,$$

where

$$I_1(\gamma)=\int_0^{2\pi}\frac{d\theta}{2\pi}|\cos\theta|^\gamma=\pi^{-1/2}G\left[\frac{\gamma}{2}+\frac{1}{2}\right]\Big/G\left[\frac{\gamma}{2}+1\right]\ ,$$

where G is the gamma function, and

$$\langle L_1^\gamma\ln L_1^\gamma\rangle=K^{3\gamma n}(I_1^{3n}\ln K^{3\gamma n}+3nI_1^{3n-1}I_2)\ ,$$

where

$$I_2(\gamma)=\int_0^{2\pi}\frac{d\theta}{2\pi}|\cos\theta|^\gamma\ln|\cos\theta|^\gamma=\gamma dI_1(\gamma)/d\gamma\ .$$

In the denominator of Eq. (42a) it is sufficient to take only the lowest-order term in $\ln K$ if we assume $\ln K\gg 1$ and $\lambda_2\sim O(1)$. Thus we do not require knowledge of L_2,

$$\langle L_1^\gamma\ln(L_1L_2)\rangle\cong\langle L_1^\gamma\rangle\ln K^{3n}\ .$$

Inserting these in Eq. (42a) we obtain

$$\tilde{D}_1=3-\frac{I_2-I_1\ln I_1}{I_1\ln K^{3\gamma}}\ . \tag{50}$$

Note that this gives $\tilde{D}_1<3$ [cf. the discussion following Eq. (22)]. Thus the measure is fractal. The *ABC* map with $K=1.5$ in Eq. (48) has been used to numerically evolve an initial vector field $\mathbf{B}(\mathbf{x},0)$ in Refs. 2 and 3. It was shown that the numerical results display a tendency for the field to concentrate in smaller and smaller fine scaled regions consistent with eventual concentration on a fractal. Note that for large K the dimension is slightly less than 3 and approaches 3 for $K\to\infty$. That the dimension approaches 3 for large K is a consequence of the fact that for large K the spread in the distribution of Lyapunov exponents becomes small compared with the average exponent which is of order $\ln K$. Applying the same technique to the passive scalar case we find that the information dimension of μ_ϕ [given by Eq. (44)] is the same as that for μ_B, Eq. (50), for $\ln K\gg 1$.

V. NONIDEAL EFFECTS

A. Effect of Diffusion on Passive Scalar Gradients

We can qualitatively understand the role of diffusion by considering the following argument. In the absence of diffusion the value of a passive scalar ϕ at any point and time $(\mathbf{x},t)$ is determined by the value that ϕ had at the initial point $(\mathbf{x}_0,0)$ whose subsequent trajectory carried it to the point $\mathbf{x}$. Similarly, from Eq. (6b) the gradient of ϕ can be expressed in terms of the initial gradient on the same trajectory. In the presence of diffusion the value of ϕ at some point becomes a weighted average of the initial values of ϕ with the weighting being a Green's function. The Green's function $\hat{G}(\mathbf{x}',t';\mathbf{x},t)$ satisfies the equation

$$\frac{\partial \hat{G}}{\partial t'}+\mathbf{v}(\mathbf{x}',t')\cdot\frac{\partial}{\partial \mathbf{x}'}\hat{G}=-\xi\frac{\partial}{\partial \mathbf{x}'}\cdot\frac{\partial \hat{G}}{\partial \mathbf{x}'} , \tag{51}$$

with $t'\leq t$ and the "initial" condition taken at $t'=t$ to be

$$\hat{G}(\mathbf{x}',t;\mathbf{x},t)=\delta(\mathbf{x}'-\mathbf{x}) .$$

When the diffusion coefficient is small and time is not too large, the Green's function will be strongly peaked around the initial point on the trajectory $(\mathbf{x}_0,0)$ and the value of ϕ and its gradient can be calculated as if the diffusion coefficient were strictly zero. This approximation will break down for large enough time such that the Green's function acquires a width which is comparable to the initial scale length for variations of ϕ. At this time $|\nabla\phi|$ will cease to grow exponentially.

To estimate this time, we consider the evolution equation for the typical separation between two points $\boldsymbol{\delta}$ which are convected by the fluid and diffuse,

$$\frac{d}{dt'}|\boldsymbol{\delta}|^2=-2\xi+2h_m|\boldsymbol{\delta}|^2 ,$$

where ξ is the diffusion coefficient and $h_m<0$ is the most negative Lyapunov exponent corresponding to trajectories which diverge as they are traced backwards. The variable t' runs backward from the current time t to the initial time 0 (since both -2ξ and $2h_m|\boldsymbol{\delta}|^2$ are negative, they both lead to increase of $|\boldsymbol{\delta}|^2$ as t' runs backward). If we take $\boldsymbol{\delta}(t'=t)=0$ as the initial condition, then the magnitude of $\boldsymbol{\delta}$ at $t'=0$ can be thought of as being the extent of the Green's function. The solution,

$$|\boldsymbol{\delta}(0)|^2=\frac{\xi}{|h_m|}[\exp(2|h_m|t)-1] , \tag{52}$$

thus gives the extent of the Green's function. When this equals the initial scale length l_0, exponential growth of the gradient ceases. Equating $\delta(0)$ and l_0, we find that the time t for which we can neglect diffusion is given by

$$t<t_\xi=\frac{1}{2|h_m|}\ln(|h_m|l_0^2/\xi) . \tag{53}$$

For times less than t_ξ the gradient of ϕ will grow exponentially at a rate $|h_m|$. The typical scale length of ϕ at t_ξ is given by

$$l_\xi=l_0\exp(-|h_m|t_\xi)=(\xi/|h_m|)^{1/2} , \tag{54}$$

and the maximum ratio of the final gradient to the initial gradient is given by

$$(l_0/l_\xi)=(|h_m|l_0^2/\xi)^{1/2} . \tag{55}$$

The effect that diffusion will have on the spectrum of fractal dimensions can be treated using the distribution of Lyapunov exponents discussed in Sec. III C. For a two-dimensional continuous time system we expect

$$p(h,t)\sim[tG''(h)/2\pi]^{1/2}\exp[-tG(h)]$$

in the absence of diffusion. With diffusion present there will be a cutoff forcing $p(h,t)$ to effectively zero for exponents (equivalently, length scales) such that $h>h_c$, where h_c satisfies

$$h_ct=\tfrac{1}{2}\ln\left[\frac{hl_0^2}{\xi}\right] . \tag{56}$$

This cutoff will not affect the spectrum of dimensions $D_q(\gamma)$ provided that the stationary phase points $h=\xi_\gamma$ and $h=\xi_\sigma$ defined by Eq. (32) and appearing in Eq. (34) are smaller than h_c. For large enough time, h_c will become smaller than ξ_γ and ξ_σ and the dimension of the measure will cease to be described by our theory. This time will depend on γ and q.

The preceding discussion applies to the initial value problem where an initially smooth $\phi(\mathbf{x})$ acquires small scales due to the chaotic fluid flow. In the quasisteady problem one imagines that a steady smooth source $S(\mathbf{x})$ with scale length l_0 is added to the right-hand side of Eq. (2), and the time asymptotic properties of the measure are of interest. The value of ϕ and its gradient can be obtained using the same Green's function as introduced for the initial value problem. In particular

$$\phi(\mathbf{x},t)=\int d\mathbf{x}'\int_{-\infty}^{t}dt'S(\mathbf{x}')\hat{G}(\mathbf{x}',t';\mathbf{x},t) , \tag{57}$$

where $S(\mathbf{x}')$ is the source term. The difference between the values of $\phi(\mathbf{x},t)$ on two adjacent points separated by $\delta\mathbf{x}$ can be expressed as a convolution of the source with the difference of the Green's function,

$$\delta\phi=\int_{-\infty}^{t}dt'\int d\mathbf{x}'S(\mathbf{x}')\delta\mathbf{x}\cdot\frac{\partial}{\partial\mathbf{x}}\hat{G}(\mathbf{x}',t';\mathbf{x},t) . \tag{58}$$

For times in the recent past, i.e., $t-t'<t_\xi$, the integrand in Eq. (58) grows exponentially as

$$\delta\mathbf{x}(t')\cdot\nabla S(\mathbf{x}(t')) ,$$

where $\delta\mathbf{x}(t')$ is the separation between the two trajectories leading to the final points. When the difference time $t-t'$ reaches t_ξ, the integrand tends to zero rapidly due to the exponential growth of the extent of the Green's function. Thus, if we cut off the time integral for $\delta\phi$ at $(t-t')=t_\xi$, we obtain the following estimate for the difference in the two values of ϕ:

$$\delta\phi\simeq\frac{1}{h_m}|\delta\mathbf{x}|\,|\nabla S|\exp(|h_m|t_\xi) , \tag{59}$$

where $\delta\mathbf{x}$ is the separation at $t'=t$. Dividing through by $|\delta\mathbf{x}|$ and inserting the expression for t_ξ yields an expression for the gradient of ϕ,

$$|\nabla\phi|\simeq\left[\frac{l_0^2|h_m|}{2\xi}\right]^{1/2}\frac{|\nabla S|}{|h_m|} \tag{60}$$

This estimate has the following properties. First, the local rate of dissipation $\xi|\nabla\phi|^2$ is independent of the diffusion coefficient ξ. Second, $|\nabla\phi|$ depends only on the inverse power of h_m rather than exponentially. Thus for the steady source problem and smooth flows where h_m is relatively constant in space we do not expect the measure of the dissipation to be fractal in steady state ($t > t_\xi$). In this case we have shown that ϕ is varying on small scale [Eq. (60)] on a set of dimension 2.

B. Effect of Diffusion on Convected Vector Fields

In this section we wish to consider the effect of finite resistivity on magnetic field evolution in a situation which yields a kinematic magnetic dynamo. In this case, Eq. (4) is modified by the addition of a diffusive term $\xi\nabla^2\mathbf{B}$ on its right-hand side. For simplicity in this section, we shall only consider the specific case of $q=\gamma=1$, and we shall, in addition, specialize to the following baker's map which has been discussed in Refs. 2 and 3 as a simple model of a three-dimensional time periodic flow which yields a kinematic magnetic dynamo

$$x_{n+1}=\begin{cases}\alpha x_n, & \text{if } y_n<\alpha\\ \beta x_n, & \text{if } y_n>\alpha\end{cases} \tag{61a}$$

$$y_{n+1}=\begin{cases}y_n/\alpha, & \text{if } y_n<\alpha\\ (y_n-\alpha)/\beta, & \text{if } y_n>\alpha\end{cases} \tag{61b}$$

where $\alpha+\beta=1$. The action of the map is as follows. The unit square, $0\le(x,y)\le 1$, is divided into two rectangles by a horizontal line at $y=\alpha$. The lower rectangle is compressed in the x direction by a factor α and expanded in the y direction by a factor $1/\alpha$. The upper rectangle is compressed in x by a factor $\beta=1-\alpha$ and expanded in y by $1/\beta$. (See the first two panels of Fig. 2.) The upper rectangle is then translated to be next to the lower rectangle [i.e., the up-down and left-right flipping of the upper rectangle in Eq. (23) is not done].

We add diffusion to the Baker's map (61) in the following way. We imagine that we apply the mapping (61) periodically in time at intervals of length T. When the map operation is applied, we imagine that the flow motion moving the fluid (cf. Refs. 2 and 3) is done so rapidly that negligible diffusion occurs (i.e., it takes essentially zero time to carry out the map operation). The fluid then sits motionless until it becomes time to apply the map again (i.e., the time T has elapsed from the last time the map was applied). Thus the diffusive effects essentially operate only over the dead periods between the times when the map is applied. We may think of each period as consisting of applying Eq. (61) with diffusion omitted and then letting $\mathbf{B}$ evolve according to $\partial\mathbf{B}/\partial t=\xi\nabla^2\mathbf{B}$, for a time T after which the next map operation is applied, and so on. (This type of diffusion model of kinematic dynamos has been discussed by Bayly and Childress.[4])

We shall show for this case that the long-time limit of the magnetic field is *effectively* a fractal with dimension as given in Sec. III B. By "effectively," we mean that it appears as a fractal down to some minimum scale past which diffusive smearing becomes operative. Note that this situation is very different from the case of the passive scalar (Sec. V A), where we found that for any range of scales considered the diffusion always matters if we wait long enough.

To proceed we must first recall the action of the baker's map (61) in the absence of diffusion.[2,3] Say $\mathbf{B}(x,y,\,n=0)=\hat{\mathbf{y}}B_0$, $B_0>0$, as in Sec. III B. After 2^n applications of the map there will be 2^n strips of varying widths $\alpha^{n-m}\beta^m$ ($m=0,1,2,\ldots,n$). Each strip will have the same flux, $\int_{\text{strip}}B(x,n)dx$, equal to B_0 the initial flux across the square, due to the frozen in condition, and all these fluxes will be directed upward. Thus the flux across the whole square is 2^nB_0, and we see that the flux grows exponentially in time at a rate $(\ln 2)/T$. (The exponential increase of flux makes this a kinematic dynamo.[2,3]) The number of strips of width $\alpha^{n-m}\beta^m$ is $Z(m,n)$ as discussed in Sec. III B. For large n, $Z(m,n)$ as a function of m/n is strongly peaked around $m/n=\frac{1}{2}$ with a width $O(1/\sqrt{n})$. Thus for large n most of the 2^n strips have $m/n\cong 1/2$ and width of order $(\alpha\beta)^{n/2}$. The information dimension ($q=1$) for $\gamma=1$ may be obtained in the following simple way.[2,3,5] Let $\varepsilon=(\alpha\beta)^{n/2}$, and cover a fraction $\theta<1$ (e.g., $\theta=0.9$, say) of the flux with the smallest number of x intervals of length ε. Since most of the strips obtained from iterating the map (i.e., most of the flux) have width of order $(\alpha\beta)^{n/2}$, the number $N(\varepsilon)$ of intervals of length ε needed to cover some fixed fraction θ of the flux is of the order of the total number of strips, $N(\varepsilon)\sim 2^n$. The information dimension of the magnetic field can then be obtained as[2,3,5]

$$\tilde{D}_1=1+\lim_{\varepsilon\to 0}\frac{\ln N(\varepsilon)}{\ln\varepsilon^{-1}}\ , \tag{62a}$$

where the one corresponds to the dimension along y and $\varepsilon\to 0$ corresponds to $n\to\infty$ which yields

$$\tilde{D}_1=1+\frac{\ln 2}{\ln(\sqrt{\alpha\beta})^{-1}}\ . \tag{62b}$$

This expression has been previously quoted in Sec. III B (see also Refs. 2 and 3). [Note[5] that (62) gives $\tilde{D}_1$ for $0<\theta<1$. If $\theta=1$ the right-hand side of (62a) is $\tilde{D}_0$ rather than $\tilde{D}_1$.]

We now ask, what is the effect of diffusion on the above? During each period, the map operation increases the magnetic field (by $1/\alpha$ and $1/\beta$ for $y\lessgtr\alpha$) and reduces its scale of variation (by α and β for $y\lessgtr\alpha$), after which diffusion smears the result over a length of order $\sqrt{\xi T}$. For most strips, the diffusion balances the reduction of scale at the time n specified by $\sqrt{\xi T}\sim(\alpha\beta)^{n/2}$, or

$$n_\xi\sim\ln(\xi T)/\ln(\alpha\beta)\ .$$

For longer times $n\gg n_\xi$, we expect $B(x,n)$ to approach an eigenfunction of the map-diffusion operator,

$$B(x,n)\cong 2^n b(x)\ , \tag{63}$$

where the eigenfunction $b(x)$ has a minimum scale $\sqrt{\xi T}$. Say we cover the x interval (0,1) with ε intervals, and determine the minimum number of these needed to cover θ of the flux in the eigenfunction $b(x)$. We claim that $N(\varepsilon)$ has the same scaling as indicated in Eq. (62) provided that ε is not too small; that is, we have the scaling

$$N(\varepsilon)\sim\varepsilon^{(\tilde{D}_1-1)}\ , \tag{64}$$

for $\varepsilon\gtrsim\sqrt{\xi T}$, where $\tilde{D}_1$ is given by Eq. (62b). To see that this is the case imagine that we initialize the magnetic field in the eigenfunction $b(x)$ and consider a succession of ε values $\varepsilon=(\alpha\beta)^{p/2}$ where p is an integer with

$1 \ll p < n_\xi$; note that these ε values are larger than the diffusive scale. Now evolve the field forward p steps. The initial flux [namely, $\Phi_0 = \int_0^1 b(x)dx$] is now in each of 2^p strips of varying widths $\alpha^{p-m}\beta^m$ and most of these have widths of order $(\alpha\beta)^{p/2}$. [Because $(\alpha\beta)^{p/2} \gg \sqrt{\xi T}$ diffusion has negligible effect on this statement.] Thus the number of intervals to cover a fraction $\theta < 1$ of the flux is as given previously (namely, $\sim 2^p$), and the arguments leading to Eq. (62) apply. However, by Eq. (63) we have that $B(x,p) \cong 2^p b(x)$. Thus since the factor 2^p does not change the fractal dimension $b(x)$ must satisfy Eq. (64), and it appears as an effective fractal quantity with $\tilde{D}_1$ given by Eq. (62b) for scales larger than $\sqrt{\xi T}$.

To conclude this section, we emphasize that our result that $\tilde{D}_1$ applies for the small diffusion case is only in the specific context of our baker's map example, Eq. (61), and we do not know what happens in general. For example, in Eq. (61) there are no reversals of flux (i.e., if the initial **B** is everywhere upward it remains so), while the map (23) reverses flux on each iterate. Thus for Eq. (23) (which is not a dynamo[3]), as time proceeds it can be shown[3] that there is an ever more fine-scaled spatial alternation between upward and downward field vectors. Small diffusion eventually leads to mutual cancellation effects when the upward and downward vector regions diffuse into each other. This effect is not present for the case of Eq. (61), and its absence is what allows the simple analysis we have given above.

VI. CONCLUSIONS

Motivated by recent work on magnetic dynamos and by the possibility of experimentally measuring gradients of convected passive scalars,[7] we have considered the convection of vector fields and scalar functions by incompressible, chaotic fluid flows. We have defined measures based on the magnitudes of the vectors and the gradients of scalars. These measures have been shown to be multifractals. The dimension spectra for these fractal measures have been related to the stretching properties of the fluid flows by a partition function formalism, and the utility of this formalism has been demonstrated by application to examples.

ACKNOWLEDGMENTS

This work was supported by the U.S. Department of Energy and by the Office of Naval Research (Physics Program). We thank John M. Finn for discussions.

[1] Some recent works on the convection of passive scalars in chaotic flow fields are the following: H. Aref, J. Fluid Mech. **143**, 1 (1984); T. Dombre, U. Frisch, J. M. Greene, M. Henon, A. Mehr, and A. M. Soward, *ibid.* **167**, 353 (1986); J. Chaiken, C. K. Chu, M. Tabor, and Q. M. Tran, Phys. Fluids **30**, 687 (1987); D. V. Khakhar, H. Rising, and J. M. Ottino, J. Fluid Mech. **172**, 419 (1986); S. W. Jones and H. Aref, Phys. Fluids **31**, 485 (1988); T. H. Solomon and J. P. Gollub, *ibid.* **31**, 1372 (1988).

[2] J. M. Finn and E. Ott, Phys. Rev. Lett. **60**, 760 (1988).

[3] J. M. Finn and E. Ott, Phys. Fluids **31**, 2992 (1988), and references therein.

[4] V. I. Arnol'd, Ya. B. Zeldovich, A. A. Ruzmaikin, and D. D. Sokoloff, Zh. Eksp. Teor. Fiz. **81**, 2052 (1981) [Sov. Phys.—JETP **56**, 1083 (1981)]; B. J. Bayly and S. Childress, Phys. Rev. Lett. **59**, 1573 (1987); D. Galloway and U. Frisch, Geophys. Astrophys. Fluid Dyn. **36**, 53 (1986); H. K. Moffat and M. R. E. Proctor, J. Fluid Mech. **154**, 493 (1985); H. R. Strauss, Phys. Rev. Lett. **57**, 2231 (1986).

[5] J. D. Farmer, E. Ott, and J. A. Yorke, Physica D **7**, 153 (1983).

[6] B. B. Mandelbrot, J. Fluid Mech. **62**, 331 (1974); C. Meneveau and K. R. Sreenivasan, in *Physics of Chaos and Systems Far from Equilibrium,* edited by M.-D. Van and B. Nichols (North-Holland, Amsterdam, 1987); R. Benzi, G. Paladin, G. Parisi and A. Valpiani, J. Phys. A **17**, 3521 (1984); U. Frisch and G. Parisi, in *Turbulence and Predictability in Geophysical Fluid Dynamics and Climate Dynamics,* edited by M. Ghil, R. Benzi, and G. Parisi (North-Holland, New York, 1985), p. 84.

[7] R. R. Prasad, C. Meneveau, and K. R. Sreenivasan, Phys. Rev. Lett. **61**, 74 (1988).

[8] A. Renyi, *Probability Theory* (Elsevier North-Holland, Amsterdam, 1970); P. Grassberger, Phys. Lett. **97A**, 227 (1983); H. G. E. Hentshel and I. Procaccia, Physica D **8**, 435 (1983).

[9] P. Grassberger, Phys. Lett. **107A**, 101 (1985); T. C. Halsey, M. J. Jensen, L. P. Kadanoff, I. Procaccia, and B. I. Shraiman, Phys. Rev. A **33**, 1141 (1986).

[10] R. Badii and A. Politi, Phys. Rev. A **35**, 1288 (1987); T. Morita, H. Hata, H. Mori, T. Horita, and K. Tomita, Prog. Theor. Phys. **78**, 511 (1987); C. Grebogi, E. Ott, and J. A. Yorke, Phys. Rev. A **37**, 1711 (1988).

[11] P. Grassberger, R. Badii, and A. Politi, J. Stat. Phys. **51**, 135 (1988); E. Ott, C. Grebogi, and J. A. Yorke, Phys. Lett. (to be published); E. Ott, T. Sauer, and J. A. Yorke, Phys. Rev. A (to be published).

[12] The quantity $\langle L_1^q \rangle$ appearing in the ratio (19a) has been discussed by H. Fujisaka, Prog. Theor. Phys. **71**, 513 (1984).

[13] K. Binder and A. P. Young, Rev. Mod. Phys. **58**, 801 (1986).

[14] M. Feingold, O. Piro, and L. P. Kadanoff, J. Stat. Phys. **50**, 529 (1988).

[15] B. V. Chirikov, Phys. Rep. **52**, 263 (1979).